Appl. Phys. A 61, 111–114 (1995)

Applied Physics A Materials Science & Processing

X-ray absorption spectroscopy study of pulsed-laser-evaporated amorphous carbon films

A. Gutiérrez[1,*], **J. Díaz**[2], **M. F. López**[1,*]

[1] Institut für Experimentalphysik, Arnimallee 14, D-14195 Berlin, Germany
[2] E.S.R.F., B.P. 220, F-38043 Grenoble, France

Received: 16 March 1995 / Accepted: 10 April 1995

Abstract. Amorphous carbon (a–C) films obtained by pulsed-laser ablation of graphite have been investigated by X-ray Absorption Spectroscopy (XAS). The onset of $1s \rightarrow \sigma^*$ transitions in the films lies in the gap between the π^* and σ^* bands in graphite and very close to the absorption edge of diamond, indicating a high content of sp^3 hybridization. A sharp feature at this onset is observed and assigned to a core exciton in sp^3-hybridized disordered C atoms. Its shift of 0.5 eV with respect to the core exciton in diamond is probably due to a higher localization of the excited electron induced by disorder. A small peak coming from C–H bonds at the surface is observed and its intensity increases with the amount of sp^3-hybridized atoms in the sample. This can be easily explained by associating a higher amount of dangling bonds at the surface to a higher sp^3 content. Polarization-dependent XAS measurements show that the angular distribution of these C–H bonds has a mean value close to the normal to the surface.

PACS: 81.15.Fg; 68.55.Nq; 71.25.Mg; 82.65.My

Amorphous carbon films (a–C) with a high content of sp^3 hybridization, also called "diamond-like" films, are technologically very important due to their similar properties to diamond, like hardness, chemical inertness, very low electrical conductivity and wide band gap [1, 2], having, in addition, the possibility to easily accept impurity donors, like nitrogen [3] or phosphorous [4]. Preparation of these a–C films usually involves atomic or ionic beams with moderate energies produced by a variety of methods like cathodic carbon arcs [5], rf sputtering [6] or rf-assisted plasma deposition [7, 8]. The possibility to prepare very thin films of these materials makes them very interesting for applications in microelectronics, where integration of small-sized elements is playing a crucial role. Recently, epitaxially grown ultrathin diamond-like films have been obtained by laser ablation of graphite [9]. Laser-assisted evaporation of graphite produces high quality a–C films with a very low hydrogen content [10, 11]. The quality of the films is given by the ratio of sp^3 to sp^2 hybridization, and depends on a variety of parameters, like laser power, laser wavelength, angle between target and sample, thickness of the films, etc. [12, 13]. XAS is a standard technique to investigate chemical and electronic properties of materials [14]. Its site and symmetry selectivity can also give information about bonding lengths and angles. In the case of carbon-containing species, the ratio of sp^3 to sp^2 hybridization can be easily determined because $1s \rightarrow \pi^*$ and $1s \rightarrow \sigma^*$ transitions in sp^2-coordinated atoms are well separated in energy from $1s \rightarrow \sigma^*$ transition in atoms with sp^3 hybridization. This makes XAS a very good tool to characterize a–C films.

In this paper, we report on a XAS study of a–C films prepared by pulsed-laser evaporation of graphite. Samples were prepared under high-vacuum conditions using a Nd:YAG laser beam focused onto a graphite target. This produces a high-energy carbon beam, or plume, consisting of a mixture of neutral and charged atoms and clusters. We used a laser power of 10^{10} W/cm^2, with 20 ns pulses carrying an energy density of 250 mJ/cm^2. A Si(100) crystal was used as substrate. These parameters have already proved to give films with good quality and high sp^3/sp^2 ratio, as demonstrated by previous Raman, Auger, EELS, and STM studies [9, 12, 13]. The density of neutral and charged particles and their mean kinetic energy depend on the angle of the substrate with respect to the normal to the target φ, being maximum for φ=0° [13]. Four samples were prepared with substrates placed at angles φ = 0, 20, 45 and 70°, respectively. Another sample at φ=0° was grown using a neutral C beam produced by removing the plasma content of the plume by means of an electric field normal to the beam trajectory. The thickness of the films ranged between 1000 Å for φ = 70° and 2500 Å for φ = 0°. XAS measurements were performed at the SX700/II monochromator of the Berliner Elektronenspeicherring für Synchrotronstrahlung (BESSY) in Total Electron Yield mode (TEY). The resolution was set to $\approx$ 150 meV at the C-1s absorption edge. Additionally to the a–C films, a Highly Oriented Pyrolitic Graphite sample (HOPG) and a diamond film grown by Chemical Vapour Deposition (CVD) were measured as references.

Figure 1 shows XAS spectra of the HOPG sample (a), the CVD-diamond sample (b), as well as four a–C films grown at

Present address: CENIM, Avda. Gregorio del Amo 8, E-28040 Madrid, Spain (Fax: +34-91/534-7425)

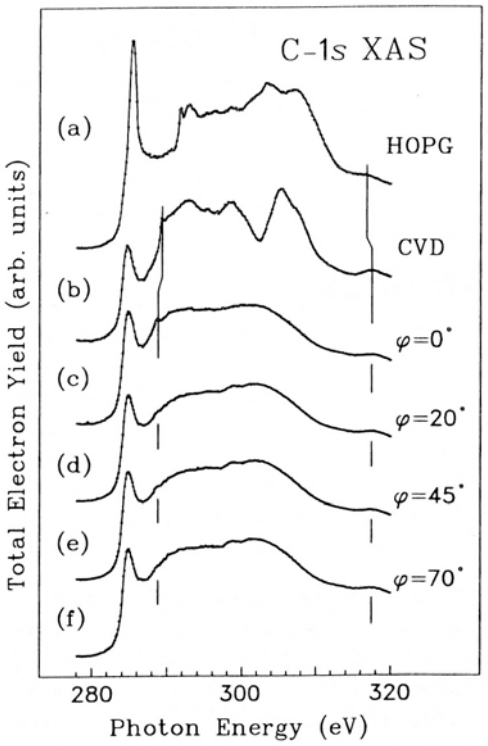

Fig. 1. X-ray absorption spectra in TEY mode of a highly oriented pyrolitic graphite sample (*a*), a CVD-diamond film (*b*), and four a–C films prepared with a laser power of 10^{10} W/cm^2 and at angles with respect to the graphite target of $\varphi = 0°$ (*c*), $\varphi = 20°$ (*d*), $\varphi = 45°$ (*e*), and $\varphi = 70°$ (*f*)

different angles with respect to the graphite target (c–f). The angle between the electric vector of the incident light and the normal to the surface was 90° and secondary electrons leaving the surface at 45° from the normal were collected. Spectra (a) and (b) show well-defined features similar to other spectra previously reported [15, 16]. In graphite, the onset of $1s \rightarrow \pi^*$ transitions lies at $\approx$ 285 eV while $1s \rightarrow \sigma^*$ transitions start at $\approx$ 291 eV. In diamond, the onset of σ^* states lies in the gap between π^* and σ^* states in graphite, i.e., at $\approx$ 289 eV. CVD-diamond films usually consist of small diamond crystallites embedded in an amorphous or graphitic carbon matrix made of sp^2-hybridized atoms. The first broad peak at 284.6 eV in spectrum (b) seems to originate from $1s \rightarrow \pi^*$ transitions in the sp^2-hybridized atoms of this amorphous matrix. Note the asymmetry of this peak and its shift of $\approx$ 0.7 eV to lower energies with respect to graphite, typical of amorphous sp^2 carbon. Another feature observed in spectrum (b) and not present in pure diamond is the shoulder at $\approx$ 288 eV, just below the σ^* edge. Other authors have interpreted similar features in the XAS spectrum of CVD diamond and a–C films to C–H bonds [17], an interpretation which is further justified by the existence of C–H resonances at the same energy position in different hydrocarbons like benzene and cyclohexane [7]. The presence of these C–H bonds in the CVD diamond can be easily explained taking into account that this kind of sample is grown from hydrocarbons, so one can expect a certain amount of hydrogen in it. The shoulder at $\approx$ 288 eV in spectrum (b) is thus originated from C–H bonds in the CVD sample. The sharp peak observed at 289.2 eV has been assigned to a C-1*s* core exciton [18], though its theoretical description in the

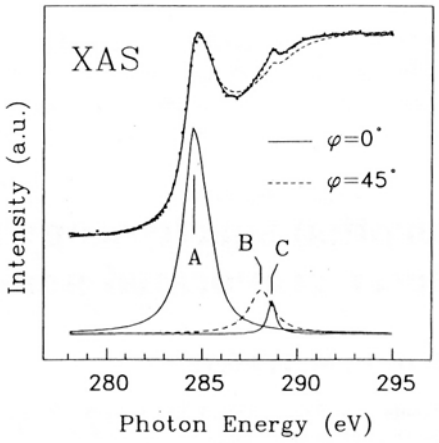

Fig. 2. Comparison of the onset of σ^* transitions in two a–C samples grown at $\varphi = 0°$ (*solid line* across data points) and $\varphi = 45°$ (*dashed line*). Both curves are the result of a least-squares fit of the experimental data using two arctangents and three Lorentz lines; the latter are shown below

equivalent-core approximation [19, 20] or in the effective-mass approximation [18, 21], is still not clear. The rest of the spectrum consists of the same structures observed in pure diamond, including the second absolute gap at $\approx$ 302 eV [18]. Spectrum (c) corresponds to an a–C sample grown at $\varphi = 0°$. The first peak at 284.6 eV is assigned to π^* states from sp^2-hybridized atoms in an amorphous matrix, and has the same shape and energy position as that observed in spectrum (b). The rest is almost featureless, except for a sharp weak peak at 288.7 eV and two broad bands centered at 293 and 302 eV. At higher angles (spectra d–f), the peak at 288.7 eV gradually decreases and the high-energy band splits into a double structure. A similar double band at around 300 eV has been assigned to graphitization of an amorphous sample at high temperatures [7]. A previous Raman study on a similar set of samples gave a higher crystallinity and a lower sp^3 content for samples grown at higher angles [13]. According to these previous results, the sample grown at $\varphi = 70°$ probably consists of small graphitic nanocrystals embedded in the amorphous matrix. The most striking feature observed in Fig. 1 is, however, the sharp peak at 288.7 eV, especially visible in spectrum (c). Since C–H resonances are much broader and lie at lower energies, we can exclude that this peak comes from C–H bonds. On the other hand, its similar lineshape and proximity to the diamond core exciton suggest that this peak can be originated by an excitonic process in amorphous, sp^3-hybridized atoms. Its observed shift of 0.5 eV with respect to the diamond exciton may be due to either a shift of the band edge position in the a–C with respect to the CVD sample, or a change in the excitonic binding energy. A similar increase in the binding energy is indeed expected in amorphous with respect to crystalline samples due to a higher localization of the excited state induced by disorder [22, 23].

There is a direct correlation between the intensity of the peak at 288.7 eV and the sp^3 content of the sample (Fig. 2). The strong intensity fall of this peak observed between spectrum (c) and spectrum (d) in Fig. 1 indicates that already for angles as small as 20° the sp^3 content of the samples is much lower than for the central sample. The intensity of this peak gradually decreases from spectrum (d) to spectrum

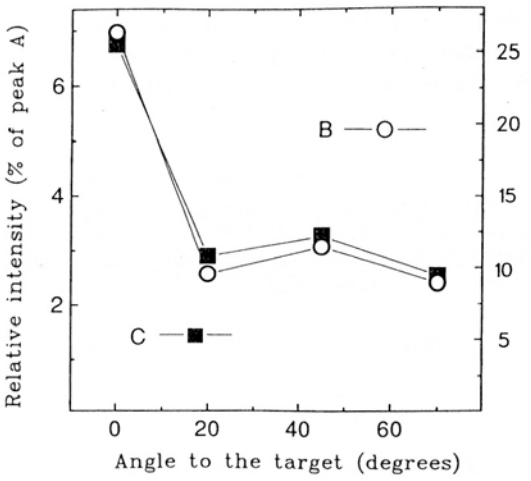

Fig. 3. Evolution of the intensity of peaks B (*empty circles, right scale*), and C (*full squares, left scale*) of Fig. 2, relative to the intensity of peak A, with respect to the angle between the normal to the target and the substrate φ

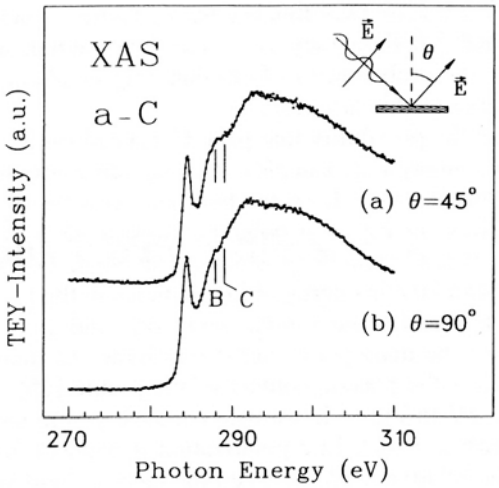

Fig. 4. Polarization dependent XAS spectra of an a–C film grown using a neutral plume, i.e., removing the plasma. θ is the angle between the electric field of the incident X-ray beam and the normal to the sample surface. The *vertical lines* show transitions to states assigned to C–H bonds (288 eV) and to an excitonic peak from sp^3-hybridized atoms (288.7), respectively

(f), which is the one with less sp^3 content, but not negligible. This can also be seen from the small peak at ≈ 318 eV, whose position is different in graphite as in the rest of the samples. At this energy the EXAFS region starts, and for a complete detailed analysis a much broader energy range is needed. However, since scattering amplitudes and phases are only element dependent, and in all cases we have the same elemente, i.e., carbon, the differences between graphite and the rest of the samples in this region may originate from differences in the bond length. If this is the case, the fact that for all a–C samples the position of this peak is the same as in spectrum (b) suggests that all of them have sp^3-coordinated atoms, even that grown at $\varphi = 70°$.

To make a more detailed quantitative analysis, we performed a least-squares fit of the data for the energy region close to the absorption edge. In Fig. 2, we show the result of such an analysis for the samples grown at $\varphi = 0°$ (solid line across the data points) and $\varphi = 45°$ (dashed line). To reproduce all spectral features we used two arctangents, centered at 285 and 288.9 eV, for the π and σ edges, respectively, and three Lorentzians, shown at the bottom of Fig. 2. The first arctangent describes the transitions from the $1s$ core level to the continuum states above the π edge in sp^2-hybridized atoms, while the second one accounts for transitions to continuum σ^* states of atoms with sp^3 hybridization. Transitions to σ^* states in sp^2-hybridized atoms would be described by an arctangent at 292.5 eV, as indicated by a similar least-squares fit of the graphite spectrum (not shown). In the case of the CVD-diamond sample, the same energy positions of the arctangents as in a–C samples describe quite well the experimental data. Additionally to the arctangents, three Lorentz lines were needed to fit the data. The first one, at 284.5 eV (labelled A in Fig. 2) accounts for the π^* resonance in the sp^2 atoms. The peak at 288.7 eV is described by the Lorentz line labelled C in Fig. 2. An extra peak at 288 eV, labelled C, has to be included in the fit in order to describe well the data points. The small intensity of this peak may induce to think that it is only an artifact of the fitting procedure. However, as it will be shown below (Fig. 4), the peak is clearly visible when another polarization angle is used in the experiment. As discussed above for the CVD diamond sample, at this energy position C–H resonances have been observed. In the case of the a–C samples, however, no hydrocarbons are used during the preparation process, in contrast to CVD diamond, but only a pure carbon beam coming from a graphite target. As already mentioned, samples were prepared under high vacuum conditions, and, consequently, there is some amount of residual gases in the vacuum chamber, especially hydrogen. Very reactive surfaces will be pasivated in a very short time by the most reactive residual gases in the chamber. Since preparation of our samples involves conditions very far away from the equilibrium, we expect many dangling bonds to be formed. In the bulk, bonds can easily rearrange in order to find the most favourable configuration, but on the surface the coordination number is lower, and, consequently, most of them remain unsaturated. Under these conditions, the residual hydrogen gas in the vacuum chamber can react with the dangling bonds at the surface and give rise to the observed peak at 288 eV. Note that the measurements were done in TEY mode, with an estimate probe depth lower than ≈ 40 Å [24], i.e., with a high surface sensitivity. It is clear from Fig. 2, that both the peak at 288.7 eV and the intensity of the transitions to σ-sp^3 states decrease from $\varphi = 0°$ to $\varphi = 45°$, as it was already clear from Fig. 1.

In Fig. 3, we show the evolution of the intensity of peaks B and C with the angle to the target φ. A big decrease of the excitonic peak C, from $\varphi = 0°$ to $\varphi = 20°$, can be observed, whereas for higher angles the intensity shows only small variations. It is interesting to note that peak B, assigned to the C–H bonds at the surface, has almost the same behaviour as peak C, associated with the sp^3 hybridization. As already discussed above, the hydrogen content of the samples is probably related to the presence of dangling bonds at the surface. This, together with the trend observed in Fig. 3, would involve that the amount of dangling bonds at the surface is related to the amount of sp^3-hybridized C atoms. This is a reasonable assumption since σ orbitals in sp^2-

hybridized carbon form two-dimensional structures, whereas in sp^3-hybridized carbon they are three-dimensional, and, consequently, the probability to form dangling bonds at the surface is higher in this last case.

To exclude the possibility that peak C, related to the sp^3 content in our amorphous samples, has the same origin as peak B, i.e., that it comes from the hydrogen content of the surface, we show in Fig. 4 a polarization-dependent XAS spectrum of an a–C sample grown without ions. For this sample, the mean kinetic energy of the particles in the plume is the same as that for the sample with ions and $\varphi = 0°$. However, since the main parameter determining the quality of the samples is the plasma content of the plume [25], the peak at 288.7 eV in Fig. 4 has a lower intensity, similar to the sample with $\varphi = 45°$. In a polarization-dependent XAS experiment the relative angle between the electric field vector of the X-ray beam **E** and the surface is varied. Since the transition probability depends upon the scalar product between **E** and the symmetry axis of the bonding, dipolar transitions from bonds arranged parallel to the electric field have a higher probability as those with other angles, while for **E** perpendicular to the symmetry axis of the bond the intensity becomes zero. This makes XAS a good tool to study the geometrical properties of materials at an atomic scale. In Fig. 4, θ is the angle between the electric field vector and the normal to the surface. For $\theta = 90°$, the electric field is parallel to the surface, and intensity from bonds normal to the surface is zero. For $\theta = 45°$ bonds normal and parallel to the surface make a contribution to the XAS signal. As is shown in Fig. 4, the peak at 288 eV shows a strong polarization dependence, while the peak at 288.7 eV does not change when θ is varied, indicating no preferred orientation in the last case, and, consequently, a different origin as that of the peak at 288 eV, assigned to C–H bonds. The increase in intensity of peak B when θ decreases involves that the C–H bonds align close to the normal to the surface, but not completely normal since in that case the intensity of this peak for $\theta = 90°$ would be zero. This arrangement of the C–H bonds can be easily understood assuming that the dangling bonds at the surface are more likely aligned away from the sample surface, since bonds parallel to the surface have other C atoms around to become saturated. Assuming an angle distribution of the C–H bonds around a mean value, a quantitative estimation of this value based on the observed intensity variation of the peak at 288 eV can be made, giving 20° with respect to the normal to the surface.

In summary, we have presented an X-ray absorption study of several amorphous "diamond-like" films prepared by pulsed-laser evaporation of a graphite target. The quality of the samples can be estimated by looking at the intensity of the $1s \rightarrow \sigma^*$ transitions. The sp^3 content of the samples changes with the angle between substrate and graphite target during deposition, strongly decreasing for angles apart from the normal, where the ionic content of the plume is lower. C–H bonds are found at the surface as a consequence of the presence of dangling bonds. Since samples with higher content of sp^3-hybridized atoms have a higher degree of dislocations, and, consequently, a higher amount of dangling bonds, they have more hydrogen content at the surface than samples with lower quality. The polarization dependence of the C–H resonance gives an angle distribution of the C–H bonds with a mean value of 20° with respect to the normal to the surface.

Acknowledgements. We thank Salvador Ferrer and Fabio Comin for fruitful discussions as well as technical assistance during sample preparation. Technical assistance at BESSY by Eduardo Navas and Sergei Molodtsov is also appreciated. A. G. and M. F. L. thank the spanish Ministerio de Educación y Ciencia for financial support.

References

1. P. J. Fallon, V. S. Veerasamy, C. A. Davis, J. Robertson, G. A. J. Amaratunga, W. I. Milne, J. Koskinen: Phys. Rev. B **48**, 4777 (1993)
2. J. Robertson: Phys. Rev. Lett. **68**, 220 (1992)
3. V. S. Veerasamy, J. Yuan, G. A. J. Amaratunga, W. I. Milne, K. W. R. Gilkes, M. Weiler, L. M. Brown: Phys. Rev. B **48**, 17954 (1993)
4. V. S. Veerasamy, G. A. J. Amaratunga, C. A. Davis, A. E. Timbs, W. I. Milne, D. R. McKenzie: J. Phys. **5**, L169 (1993)
5. D. R. McKenzie, D. Muller, B. A. Pailthorpe: Phys. Rev. Lett. **67**, 773 (1991)
6. D. Dasgupta, F. Demichelis, C. F. Pirri, A. Tagliaferro: Phys. Rev. B **43**, 2131 (1991)
7. G. Comelli, J. Stöhr, C. J. Robinson, W. Jark: Phys. Rev. B **38**, 7511 (1988)
8. J. Fink, T. Müller-Heinzerling, J. Pflüger, A. Bubenzer, P. Koidl, G. Crecelius: Solid State Commun. **47**, 687 (1983)
9. J. A. Martín, L. Vázquez, P. Bernard, F. Comin, S. Ferrer: Appl. Phys. Lett. **57**, 1742 (1990)
10. D. L. Pappas, K. L. Saenger, J. Bruley, W. Krakow, J. Cuomo, T. Gu, R. W. Collins: J. Appl. Phys. **71**, 5675 (1992)
11. F. Xiong, Y. Y. Wang, V. Leppert, R. P. H. Chang: J. Mater. Res. **8**, 2265 (1993)
12. J. A. Martín-Gago, J. Fraxedas, S. Ferrer, F. Comin: Surf. Sci. **260**, L17 (1992)
13. J. Díaz, J. A. Martín Gago, S. Ferrer, F. Comin, L. Abello, G. Lucazeau: Diamond Relat. Mater. **1**, 824 (1992)
14. See, for example, F. M. F. de Groot: J. Electron Spectrosc. Relat. Phenom. **67**, 529 (1994)
15. R. A. Rosenberg, P. J. Love, V. Rehn: Phys. Rev. B **33**, 4034 (1986)
16. Y. Ma, N. Wassdahl, P. Skytt, J. Guo, J. Nordgren, P. D. Johnson, J.E. Rubensson, T. Boske, W. Eberhardt, S. D. Evan: Phys. Rev. Lett. **69**, 2598 (1992)
17. K. Edamatsu, Y. Takata, T. Yokoyama, K. Seki, M. Tohnan, T. Okada, T. Ohta: Jpn. J. Appl. Phys. **30**, 1073 (1991)
    Y. Takata, K. Edamatsu, T. Yokoyama, K. Seki, M. Tohnan, T. Okada, T. Ohta: Jpn. J. Appl. Phys. **28**, L1282 (1989)
18. J. F. Morar, F. J. Himpsel, G. Hollinger, G. Hughes, J. L. Jordan: Phys. Rev. Lett. **54**, 1960 (1985)
19. Y. Ma, P. Skytt, N. Wassdahl, P. Glans, D. C. Mancini, J. Guo, J. Nordgren: Phys. Rev. Lett. **71**, 3725 (1993)
20. J. Nithianandam: Phys. Rev. Lett. **69**, 3108 (1992)
21. P. E. Batson: Phys. Rev. Lett. **70**, 1822 (1993)
22. F. Evangelisti, F. Patella, R. A. Riedel, G. Margaritondo, P. Fiorini, P. Perfetti, C. Quaresima: Phys. Rev. Lett. **53**, 2504 (1984)
23. A. Gutiérrez, M. F. López: Phys. Rev. Lett. (submitted)
24. M. Abbate, J. B. Goedkoop, F. M. F. de Groot, M. Grioni, J. C. Fuggle, S. Hofmann, H. Petersen, M. Sacchi: Surf. Interface Anal. **18**, 65 (1992)
25. J. Díaz, S. Ferrer, F. Comin, A. Gutiérrez, S. Molodtsov, M. F. López, G. Kaindl: Phys. Rev. B (submitted)

This article was processed by the author using the LaTeX style file *pljour2* from Springer-Verlag.